Journal of Hydroscience and Hydraulic Engineering
Vol. 25, No.1 May, 2007, 107-122

A WEAKLY NONLINEAR ANALYSIS OF BAR MODE REDUCTION PROCESS

By

Yasuharu Watanabe

Civil Engineering Research Institute for Cold Region, Sapporo, Japan

SYNOPSIS

This research incorporates the cross interference between the modes of double-row bars and alternate bars into a weakly nonlinear analysis, and aims at clarifying the degree of the cross interference between the modes. The rate of linear amplification is introduced into this model so that the same order can examine alternate bars and double-row bars. Hydraulic conditions of this analysis were set at a large width-depth ratio in which double-row bars were generated. The results of this analysis did not reproduce the results of hydraulic experiments quantitatively. However, it reproduced the qualitative characteristics of bar mode decrease process. Findings revealed that neither modes (alternate bars and double-row bars) do not grow up at the same time.

INTRODUCTION

To improve flood control, studies have been conducted on the behavior of bar formation on a riverbed, because once such sand waves form, they start to cause local scouring and make a river channel meander, promoting riverbank erosion. Conventionally, the initial growth rate during sandbar development is used to classify the meso-scale riverbed configuration. Theoretical studies on bar formation have been conducted by several researchers. Colombini et al. (1), Schielen et al. (5) and Izumi & Pornprommin (4) conducted weakly non-linear stability analysis on bar developments in straight channels. They clarified the bar formation process. However, these analyses did not consider an interaction of two modes (alternate bars and double-row bars). Various hydraulic tests (Fujita (2), Fujita et al. (3)) and numerical simulations (Takebayashi et al. (7), Teramoto & Tsujimoto (8)) have reported that under the condition in which sandbars of higher mode form during the initial period, mode reduction occurs with time. This means that there may be the situation in which a sandbar mode differs from the mode predicted by an initial growth rate for that riverbed configuration. In fact, there are river sections with hydraulic conditions under which double-row bars are thought to form but where mode reduction occurs or has occurred. This difference between the theoretical, initially predicted mode and the reduced mode that occurs with time must be addressed in planning flood control revetments and river conservation, since these are greatly influenced by riverbed micro-topography.

Watanabe & Kuwamura (9) experimented with sandbar formations by setting several hydraulic conditions under which either alternate bars or double-row bars formed. They applied a weakly nonlinear analysis to describe the sandbar development which was established by Colombini et al. (1) and tried to explain a mode reduction process of double-row bars (Watanabe & Kuwamura (10)). In this experiment, alternate bars and double-row bars were examined separately, and the analysis was simplified by neglecting any cross interference between the two modes.

Table 1: Hydraulic conditions of experiments and initial conditions of analysis

Run	$\widetilde{Q}$ cm^3/s	$\widetilde{D_0}$ cm	$\widetilde{T_f}$ min.	I_w	I_b	C_f	β	d_s	θ	Bed forms	$\widetilde{L_b}$ m	$\widetilde{Z_b}$ cm	λ	Z_b
S-10-20	1660	0.59	20	1/86	1/80	0.0069	76	0.13	0.055	D	2.42	2.1	1.17	3.56
S-10-40	1660	0.62	40	1/82	1/80	0.0084	73	0.12	0.060	D	2.66	2.1	1.06	3.39
S-10-60	1660	0.46	60	1/83	1/80	0.0034	98	0.17	0.044	D	2.56	2.2	1.10	4.78
S-10-80	1660	0.36	80	1/84	1/80	0.0016	125	0.21	0.034	D+A	3.76	2.5	0.75	6.94
S-10-120	1660	0.61	120	1/83	1/80	0.0079	74	0.12	0.059	D+A	5.83	2.6	0.48	4.26
S-10-240	1660	0.49	240	1/84	1/79	0.0040	92	0.16	0.047	A	3.30	4.8	0.86	9.80
S-10-480	1660	0.50	480	1/84	1/79	0.0043	90	0.15	0.047	A	6.60	5.2	0.43	10.40
S-10-960	1660	0.60	960	1/80	1/78	0.0078	75	0.13	0.060	A	4.88	4.3	0.58	7.17
S-20-20	3250	1.15	20	1/84	1/80	0.0136	39	0.07	0.109	D	2.70	2.1	1.05	1.83
S-20-40	3250	0.96	40	1/85	1/80	0.0078	47	0.08	0.090	D+A	2.68	2.4	1.06	2.50
S-20-60	3250	0.86	60	1/84	1/79	0.0057	52	0.09	0.082	D+A	3.53	3.7	0.80	4.30
S-20-80	3250	1.10	80	1/85	1/80	0.0118	41	0.07	0.103	D+A	5.89	3.4	0.48	3.09
S-20-120	3250	0.96	120	1/84	1/80	0.0079	47	0.08	0.091	A	5.41	4.3	0.52	4.48
S-20-240	3250	0.91	240	1/84	1/79	0.0067	49	0.08	0.086	A	7.50	5.6	0.38	6.15
S-20-360	3250	0.96	360	1/83	1/79	0.0080	47	0.08	0.092	A	6.83	4.5	0.41	4.69
S-20-840	3250	1.00	840	1/82	1/80	0.0092	45	0.08	0.097	A	8.18	5.5	0.35	5.50
S-30-20	5270	1.20	20	1/83	1/80	0.0060	38	0.06	0.115	D	4.65	2.8	0.61	2.33
S-30-40	5270	1.37	40	1/85	1/79	0.0086	33	0.06	0.129	D+A	5.40	6.1	0.52	4.45
S-30-60	5270	1.27	60	1/84	1/78	0.0070	35	0.06	0.121	A	6.00	5.2	0.47	4.09
S-30-80	5270	1.39	80	1/85	1/81	0.0090	32	0.05	0.130	A	6.30	5.2	0.45	3.74
S-30-120	5270	1.20	120	1/83	1/79	0.0060	38	0.06	0.115	A	5.48	4.7	0.52	3.92
S-30-240	5270	1.15	240	1/86	1/81	0.0051	39	0.07	0.107	A	5.78	5.3	0.49	4.61
S-30-600	5270	1.20	600	1/85	1/76	0.0058	38	0.06	0.113	A	8.40	6.1	0.34	5.08
S-40-20	7600	1.64	20	1/84	1/80	0.0072	27	0.05	0.156	D	2.87	2.1	0.99	1.28
S-40-40	7600	1.78	40	1/85	1/81	0.0091	25	0.04	0.167	A	5.70	6.3	0.50	3.54
S-40-60	7600	1.80	60	1/85	1/80	0.0094	25	0.04	0.169	A	4.39	3.6	0.64	2.00
S-40-80	7600	1.84	80	1/84	1/80	0.0102	24	0.04	0.175	A	5.78	5.1	0.49	2.77
S-40-120	7600	1.63	120	1/86	1/80	0.0069	28	0.05	0.151	A	7.80	5.4	0.36	3.31
S-40-180	7600	1.60	180	1/87	1/81	0.0065	28	0.05	0.147	A	9.45	5.2	0.30	3.25
S-40-330	7600	1.50	330	1/83	1/83	0.0056	30	0.05	0.144	A	6.80	5.8	0.42	3.87
S-50-20	10350	2.02	20	1/85	1/80	0.0072	22	0.04	0.190	A	4.80	3.1	0.59	1.53
S-50-40	10350	2.03	40	1/86	1/79	0.0072	22	0.04	0.188	A	4.20	2.6	0.67	1.28
S-50-60	10350	2.10	60	1/83	1/80	0.0083	21	0.04	0.202	A	5.03	4.0	0.56	1.90
S-50-80	10350	1.91	80	1/86	1/82	0.0060	24	0.04	0.177	A	6.38	5.1	0.44	2.67
S-50-120	10350	1.82	120	1/84	1/81	0.0053	25	0.04	0.173	A	5.93	5.5	0.48	3.02
S-50-240	10350	1.80	240	1/79	1/82	0.0055	25	0.04	0.182	A	6.68	5.6	0.42	3.11

D: Double-row bars, A: Alternate bars

The experiment showed that reduction from double-row bar mode to alternate bar mode could be explained even from experiments in which the two types of bars were examined separately.

This present study incorporates the cross interference between modes into nonlinear analysis to clarify the mutual influence of the modes in the mode reduction process.

OUTLINE OF HYDRAULIC EXPERIMENTS

Watanabe & Kuwamura (9) conducted hydraulic experiments on sandbar mode reduction from double-row bars to alternate bars. Table 1 shows the hydraulic conditions and the sandbar morphologies in the experiments. In Table 1, $\widetilde{Q}$ = discharge; $\widetilde{D_0}$ = average water depth; $\widetilde{T_f}$ = duration; I_w = water surface gradient; I_b = bed slope; C_f = drag coefficient of riverbed; $\beta = \widetilde{B}/\widetilde{D_0}$; $\widetilde{B}$ = half the channel width (=45cm); $d_s = \widetilde{d_s}/\widetilde{D_0}$; $\widetilde{d_s}$ = diameter of bed material (0.76mm); θ = dimensionless shear stress; $\lambda = 2\pi\widetilde{B}/\widetilde{L_b}$; and $Z_b = \widetilde{Z_b}/\widetilde{D_0}$. $\widetilde{L_b}$, $\widetilde{Z_b}$ = the average wavelength and wave height of sandbars in the observed section of channel. After reaching an equilibrium as double-row bars, the bars transform into alternate bars during a transition period. Both double-row bars and alternate bars formed in the tests S-10-80, S-10-120, S-20-40, S-20-60, S-20-80, and S-30-40. Therefore, the average wavelengths and wave heights in these tests are the average for double-row bars and alternate bars. The last number of each test name indicates a duration of water flow in minutes. The sand bars of all the experiments submerged except Run S-10. Since S-10 has shallow water depth and emerged bars form, one needs to consider the characteristics of bar forms which differ from the other experiments. Figure 1 and 2 show the observed bed topographies of Run S-20 and Run S-40.

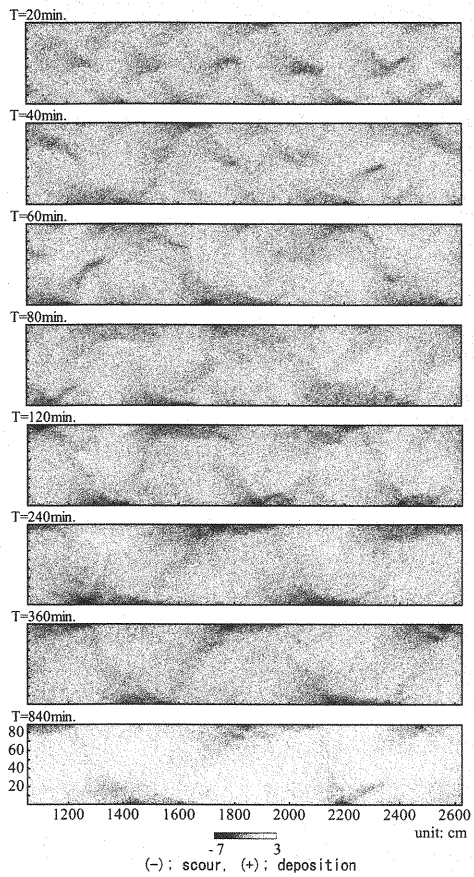

Figure 1: Observed bed topographies of Run S-20: changes in bed elevation from the initial state.

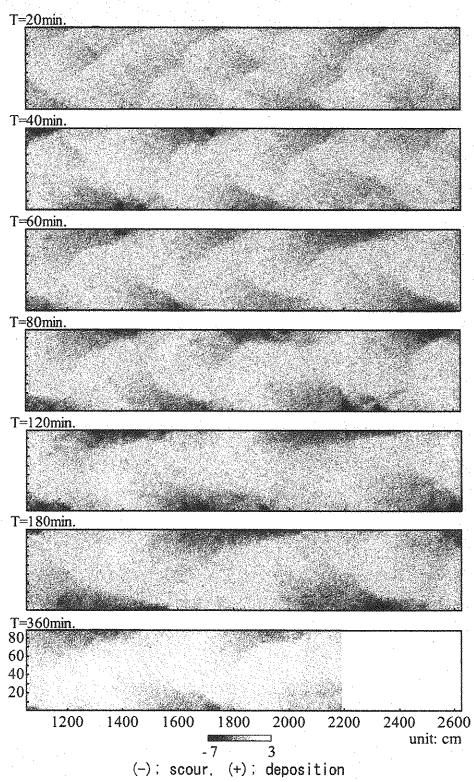

Figure 2: Observed bed topographies of Run S-40: changes in bed elevation from the initial state.

GROWTH RATE EXPANSION METHOD CONSIDERING MODE CROSS INTERFERENCE

Basic equations and dimensionless forms

Basic equations and dimensionless forms are set in the same form as Colombini et al. (1). Equations 1, 2, 3 and 4, respectively, are two steady two-dimensional shallow-water flow equations where the diffusion terms are omitted, the continuity equation, and the continuity equation of bedload, for a straight channel (width:$2\widetilde{B}$) under the coordinate system shown in Figure 3.

$$\widetilde{U}\frac{\partial \widetilde{U}}{\partial \widetilde{x}} + \widetilde{V}\frac{\partial \widetilde{U}}{\partial \widetilde{y}} + \tilde{g}\frac{\partial \widetilde{H}}{\partial \widetilde{x}} + \frac{\widetilde{\tau}_x}{\widetilde{\rho}\widetilde{D}} = 0 \tag{1}$$

$$\widetilde{U}\frac{\partial \widetilde{V}}{\partial \widetilde{x}} + \widetilde{V}\frac{\partial \widetilde{V}}{\partial \widetilde{y}} + \tilde{g}\frac{\partial \widetilde{H}}{\partial \widetilde{y}} + \frac{\widetilde{\tau}_y}{\widetilde{\rho}\widetilde{D}} = 0 \tag{2}$$

$$\frac{\partial\left(\widetilde{U}\widetilde{D}\right)}{\partial \widetilde{x}} + \frac{\partial\left(\widetilde{V}\widetilde{D}\right)}{\partial \widetilde{y}} = 0 \tag{3}$$

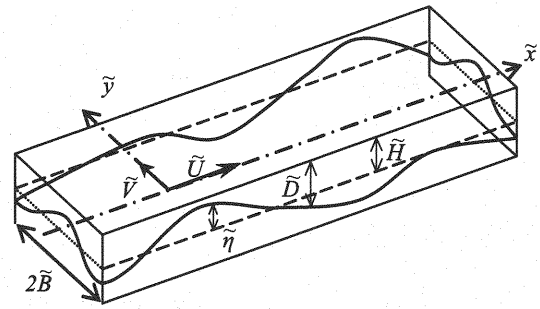

Figure 3: Definitions of coordinate system of the flow model.

$$\frac{\partial \widetilde{\eta}}{\partial \widetilde{t}} + \frac{1}{1-P}\left(\frac{\partial \widetilde{Q_{bx}}}{\partial \widetilde{x}} + \frac{\partial \widetilde{Q_{by}}}{\partial \widetilde{y}}\right) = 0 \tag{4}$$

where $\widetilde{t}$ = time; $\widetilde{x}$ = longitudinal coordinate; $\widetilde{y}$ = transverse coordinate; $\widetilde{U}$ = flow velocity in the $\widetilde{x}$ coordinate direction; $\widetilde{V}$ = flow velocity in the $\widetilde{y}$ coordinate direction; $\widetilde{H}$ = water surface level; $\widetilde{D}$ = flow depth; $\widetilde{\eta}$ = riverbed elevation $(= \widetilde{H} - \widetilde{D})$; $\widetilde{\tau_x}$ = shear stress in the $\widetilde{x}$ coordinate direction; $\widetilde{\tau_y}$ = shear stress in the $\widetilde{y}$ coordinate direction; $\widetilde{Q_{bx}}$ = bedload transport rate per unit width in the $\widetilde{x}$ coordinate direction; $\widetilde{Q_{by}}$ = bedload transport rate per unit width in the $\widetilde{y}$ coordinate direction; $\widetilde{\rho}$ = density of water; $\widetilde{g}$ = acceleration of gravity; and P = porosity of bed. Variables capped with~are dimensional.

Equations 1, 2, 3 and 4 are made dimensionless by using the parameters of uniform flow on a flat riverbed: $(U,V) = (\widetilde{U},\widetilde{V})/\widetilde{U_0}$; $D = \widetilde{D}/\widetilde{D_0}$; $H = \widetilde{H}/(F_0{}^2\widetilde{D_0})$; $(Q_{bx},Q_{by}) = (\widetilde{Q_{bx}},\widetilde{Q_{by}})/(\delta\widetilde{g}\widetilde{d_s}^3)^{1/2}$; $(\tau_x,\tau_y) = (\widetilde{\tau_x},\widetilde{\tau_y})/(\widetilde{\rho}\widetilde{U_0}^2)$; $(x,y) = (\widetilde{x},\widetilde{y})/\widetilde{B}$; $t = \widetilde{t}/(\widetilde{B}/\widetilde{U_0})$; and $F_0 = \widetilde{U_0}/(\widetilde{g}\widetilde{D_0})^{1/2}$.
Here, the suffix 0 indicates a value for uniform flow. δ = submerged specific gravity of a riverbed material. The resultant equations are as follows:

$$U\frac{\partial U}{\partial x} + V\frac{\partial U}{\partial y} + \frac{\partial H}{\partial x} + \beta\frac{\tau_x}{D} = 0 \tag{5}$$

$$U\frac{\partial V}{\partial x} + V\frac{\partial V}{\partial y} + \frac{\partial H}{\partial y} + \beta\frac{\tau_y}{D} = 0 \tag{6}$$

$$\frac{\partial (UD)}{\partial x} + \frac{\partial (VD)}{\partial y} = 0 \tag{7}$$

$$\frac{\partial \eta}{\partial t} + Q_0\left(\frac{\partial Q_{bx}}{\partial x} + \frac{\partial Q_{by}}{\partial y}\right) = 0 \tag{8}$$

where $Q_0 = (\delta d_s{}^3)^{1/2}/[F_0(1-P)]$.

Conventional perturbation method (Colombini et al. (1))

When alternate bars and double-row bars are considered separately, (U,V,H,D) in these equations are substituted by their expansions whose perturbation parameters are $\varepsilon^{1/2}$, as shown by Equations 9, 10, 11, 12 and 13.

$$\begin{aligned}(U,V,H,D) &= (1,0,H_0,1) + \varepsilon^{1/2}(U_1,V_1,H_1,D_1) \\ &\quad + \varepsilon^{2/2}(U_2,V_2,H_2,D_2) + \varepsilon^{3/2}(U_3,V_3,H_3,D_3)\end{aligned} \tag{9}$$

$$(U_1, V_1, H_1, D_1) =$$

$$\begin{cases} A_{(T)}\left(S_1 u_{111}, C_1 v_{111}, S_1 h_{111}, S_1 d_{111}\right) E_1 + c.c. & \text{for mode} = 1 \\ A_{(T)}\left(C_2 u_{121}, S_2 v_{121}, C_2 h_{121}, C_2 d_{121}\right) E_1 + c.c. & \text{for mode} = 2 \end{cases} \tag{10}$$

$$(U_2, V_2, H_2, D_2) =$$

$$\begin{cases} {A_{(T)}}^2 E_2 \left[\left(C_2 u_{222}, S_2 v_{222}, C_2 h_{222}, C_2 d_{222}\right) + \left(u_{202}, v_{202}, h_{202}, d_{202}\right)\right] + c.c. \\ +A_{(T)} \overline{A}_{(T)} \left[\left(C_2 u_{220}, S_2 v_{220}, C_2 h_{220}, C_2 d_{220}\right) + \left(u_{200}, v_{200}, h_{200}, d_{200}\right)\right] \\ + (0, 0, H_{200}, 0) & \text{for mode} = 1 \\ {A_{(T)}}^2 E_2 \left[\left(S_4 u_{242}, C_4 v_{242}, S_4 h_{242}, S_4 d_{242}\right) + \left(u_{202}, v_{202}, h_{202}, d_{202}\right)\right] + c.c. \\ +A_{(T)} \overline{A}_{(T)} \left[\left(S_4 u_{240}, C_4 v_{240}, S_4 h_{240}, S_4 d_{240}\right) + \left(u_{200}, v_{200}, h_{200}, d_{200}\right)\right] \\ + (0, 0, H_{200}, 0) & \text{for mode} = 2 \end{cases} \tag{11}$$

$$(U_3, V_3, H_3, D_3) =$$

$$\begin{cases} {A_{(T)}}^2 \overline{A}_{(T)} \left(S_1 u_{311}, C_1 v_{311}, S_1 h_{311}, S_1 d_{311}\right) E_1 + c.c. + h.h. & \text{for mode} = 1 \\ {A_{(T)}}^2 \overline{A}_{(T)} \left(C_2 u_{321}, S_2 v_{321}, C_2 h_{321}, C_2 d_{321}\right) E_1 + c.c. + h.h. & \text{for mode} = 2 \end{cases} \tag{12}$$

$$(S_m, C_m, E_n) = \left(\sin\left(\frac{1}{2}\pi m y\right), \cos\left(\frac{1}{2}\pi m y\right), \exp\left[ni\left(\lambda x - \omega t\right)\right]\right) \tag{13}$$

where, $c.c.$ = complex conjugates of the immediately preceding term; $h.h.$ = terms of the higher order; m = the mode number for transverse direction of bar formation; n = the mode number for longitudinal direction of bar formation; ω = angular frequency; and $A_{(T)}$ = the amplitude of small perturbation at time T. T is a time scale introduced to express the variation of small perturbation. The leftmost number of the three-digit suffix in Equations 10, 11 and 12 is the order, the middle number is the wave mode of small perturbation in the transverse direction, and the rightmost number is the wave mode of small perturbation in a longitudinal direction. Its relation to the time scale of flow, t, is given by Equation 14. $\overline{A}_{(T)}$ is the complex conjugate of $A_{(T)}$.

$$T = \varepsilon t \tag{14}$$

The time scale necessary for expressing development of sandbars is much greater than that for changes of water flow. On the order of $\varepsilon^{3/2}$, a modified Landau-Stuart equation shown as Equation 15 is obtained for alternate bars and double-row bars.

$$\frac{dA_{(T)}}{dT} + \alpha_1 A_{(T)} + \alpha_2 {A_{(T)}}^2 \overline{A}_{(T)} = 0 \tag{15}$$

where, α_1 and α_2 are complex coefficients expressed in terms of the amplitude of perturbations.

Equation 16 is the solution of Equation 15:

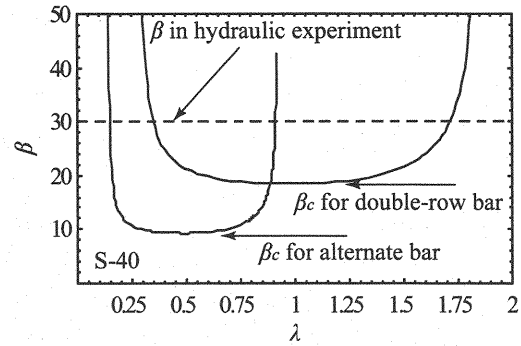

Figure 4: Neutral curves of initial growth rates calculated by the linear stability analysis.

$$|A| = \sqrt{\frac{-\mathrm{Re}(\alpha_1)}{\mathrm{Re}(\alpha_2) - a_0 \mathrm{Re}(\alpha_1) \exp[-2\mathrm{Re}(\alpha_1) T]}} \tag{16}$$

where, $|A|_0$ = assumed to be the initial amplitude of small perturbation; and a_0 = expressed by Equation 17.

$$a_0 = \frac{1}{|A|_0{}^2} + \frac{\mathrm{Re}(\alpha_2)}{\mathrm{Re}(\alpha_1)} \tag{17}$$

When the growth rate expansion method is applied to the nonlinear analysis of sandbar development, the perturbation parameter $\varepsilon^{1/2}$ is used. ε is expressed as Equation 18:

$$\beta = \beta_c (1 + \varepsilon) \tag{18}$$

where, β = actual width/depth ratio; and β_c = the minimum width/depth ratio for which the initial perturbation is neutral, i.e., whose initial growth rate is 0 in linear stability analysis.

For application of a nonlinear analysis, a width/depth ratio β needs to be close to β_c. A wavenumber of sandbar λ is given by Equation 19. To perform this analysis, however, here we assume that $\lambda_1 = 0$, because it does not greatly affect the results of the analysis.

$$\lambda = \lambda_c + \varepsilon \lambda_1 \tag{19}$$

Mode cross interference method

The growth rate expansion method was used to examine the development process of alternate bars and double-row bars on the same order. As shown in Figure 4, the critical width/depth ratio β_c, or the minimum width/depth ratio when the initial growth rate Ω_0 of a sandbar is 0, differ between alternate bar and double-row bar. In the growth rate expansion method, which describes sandbar development in a channel whose width/depth ratio is close to the critical width/depth ratio, it is theoretically impossible to simultaneously examine the growth of sandbars in channels that have different critical width/depth ratios. In addressing the mode change from double-row bar to alternate bar, one must consider the cross interference between the two modes. Thus, the alternate bar and the double-row bar need to be considered under conditions in which there is the same order of perturbation. To solve this problem, some preconditions are set as follows.

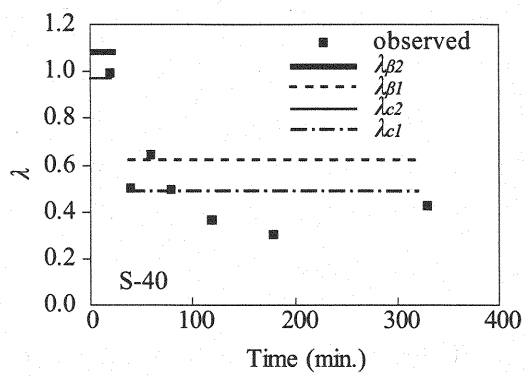

Figure 5: Changes in wavenumber of bars in hydraulic tests.

When perturbation expansion is applied to more than one type of sandbar under the condition of the same order of perturbation, a uniform perturbation parameter is required. The region in which alternate bars and double-row bars can be considered is the region that is conventionally classified as the region for double-row bars. Therefore, the analysis is applied to the case in which the critical width/depth ratio, or the minimum width/depth ratio, is β_c when the initial growth rate of a double-row bar Ω_0 is 0, and a uniform perturbation parameter is used. In this case, the critical width/depth ratio differs from that of an alternate bar, and the alternate bar has an initial growth rate that exceeds 0.

Figure 5 shows the changes in wavenumber of sand bars obtained in the previous hydraulic test on the process of reduction from double-row bar mode to alternate bar mode. The figure also contains the wavenumber λ_c at β_c obtained by linear stability analysis and the wavenumber λ_β at β obtained in the experiments. The suffix refers to the mode number. In Figure 5, the wavenumber for the alternate bar mode becomes roughly half that for the double-row bar mode as the mode reduction progresses. Thus, the wavenumber for the alternate bar mode will be assumed to have the fixed value of half that for the double-row bar mode.

When the above conditions are applied, it is impossible to satisfy equations on the first order for both the alternate bars and the double-row bars. Thus, the amplitude of the double-row bar continues to be $B_{(T)}$, a function of T, but for the alternate bar $W_{(t)}$, a function of t is used to adjust its growth rate in addition to $A_{(T)}$, a function of T, because the alternate bar mode has an initial growth rate much greater than that of double row bar in this case. This is also equivalent to changing the time scale of development in the mode 1 and the mode 2.

Accordingly, Equations 20, 21 and 22 replace Equations 9, 10, 11 and 12.

$$\begin{aligned}(U_1, V_1, H_1, D_1) = A_{(T)} W_{(t)} \left(S_1 u_{111}, C_1 v_{111}, S_1 h_{111}, S_1 d_{111}\right) E_1 + c.c. \\ + B_{(T)} \left(C_2 u_{122}, S_2 v_{122}, C_2 h_{122}, C_2 d_{122}\right) E_2 + c.c. \end{aligned} \tag{20}$$

$$
\begin{aligned}
(U_2, V_2, H_2, D_2) = {} & {A_{(T)}}^2 {W_{(t)}}^2 E_2 \left[(C_2 u_{222}, S_2 v_{222}, C_2 h_{222}, C_2 d_{222}) + (u_{202}, v_{202}, h_{202}, d_{202})\right] + c.c. \\
& + A_{(T)} \overline{A}_{(T)} W_{(t)} \overline{W}_{(t)} \left[(C_2 u_{220}, S_2 v_{220}, C_2 h_{220}, C_2 d_{220}) + (u_{200a}, v_{200a}, h_{200a}, d_{200a})\right] \\
& + {B_{(T)}}^2 E_4 \left[(C_4 u_{244}, S_4 v_{244}, C_4 h_{244}, C_4 d_{244}) + (u_{204}, v_{204}, h_{204}, d_{204})\right] + c.c. \\
& + B_{(T)} \overline{B}_{(T)} \left[(C_4 u_{240}, S_4 v_{240}, C_4 h_{240}, C_4 d_{240}) + (u_{200b}, v_{200b}, h_{200b}, d_{200b})\right] \\
& + \overline{A}_{(T)} B_{(T)} \overline{W}_{(t)} E_1 \left[(S_1 u_{211}, C_1 v_{211}, S_1 h_{211}, S_1 d_{211}) + (S_3 u_{231}, C_3 v_{231}, S_3 h_{231}, S_3 d_{231})\right] + c.c. \\
& + A_{(T)} B_{(T)} W_{(t)} E_3 \left[(S_1 u_{213}, C_1 v_{213}, S_1 h_{213}, S_1 d_{213}) + (S_3 u_{233}, C_3 v_{233}, S_3 h_{233}, S_3 d_{233})\right] + c.c. \\
& + (0, 0, H_{200}, 0)
\end{aligned}
\tag{21}
$$

$$
\begin{aligned}
(U_3, V_3, H_3, D_3) = {} & \left({A_{(T)}}^2 \overline{A}_{(T)} {W_{(t)}}^2 \overline{W}_{(t)} + A_{(T)} B_{(T)} \overline{B}_{(T)} W_{(t)}\right) E_1 \left(S_1 u_{311}, C_1 v_{311}, S_1 h_{311}, S_1 d_{311}\right) + c.c. \\
& + \left({B_{(T)}}^2 \overline{B}_{(T)} + B_{(T)} A_{(T)} \overline{A}_{(T)} W_{(t)} \overline{W}_{(t)}\right) E_2 \left(C_2 u_{322}, S_2 v_{322}, C_2 h_{322}, C_2 d_{322}\right) + c.c. \\
& + h.h.
\end{aligned}
\tag{22}
$$

where, the leftmost number of the three-digit suffix in Equations 21 and 22 is the order, the middle number is the wave mode of small perturbation in the transverse direction, and the rightmost number is the wave mode of small perturbation in the longitudinal direction. By substituting them into Equations 5, 6, 7 and 8, Equations 23 and 24 are obtained on the order of $\varepsilon^{1/2}$ (the first order):

$$
\begin{bmatrix}
p_{111,11} & p_{111,12} & p_{111,13} & p_{111,14} \\
p_{111,21} & p_{111,22} & p_{111,23} & p_{111,24} \\
p_{111,31} & p_{111,32} & p_{111,33} & p_{111,34} \\
p_{111,41} & p_{111,42} & p_{111,43} & p_{111,44}
\end{bmatrix}
\begin{bmatrix}
u_{111} \\ v_{111} \\ h_{111} \\ d_{111}
\end{bmatrix} = 0
\tag{23}
$$

$$
\begin{bmatrix}
p_{122,11} & p_{122,12} & p_{122,13} & p_{122,14} \\
p_{122,21} & p_{122,22} & p_{122,23} & p_{122,24} \\
p_{122,31} & p_{122,32} & p_{122,33} & p_{122,34} \\
p_{122,41} & p_{122,42} & p_{122,43} & p_{122,44}
\end{bmatrix}
\begin{bmatrix}
u_{122} \\ v_{122} \\ h_{122} \\ d_{122}
\end{bmatrix} = 0
\tag{24}
$$

For Equations 23 and 24 to have solutions, Determinants 25 and 26 are derived:

$$
\begin{aligned}
\begin{vmatrix}
p_{111,11} & p_{111,12} & p_{111,13} & p_{111,14} \\
p_{111,21} & p_{111,22} & p_{111,23} & p_{111,24} \\
p_{111,31} & p_{111,32} & p_{111,33} & p_{111,34} \\
p_{111,41} & p_{111,42} & p_{111,43} & p_{111,44}
\end{vmatrix}
&= f_{111(W_{(t)}, \beta_c, \lambda_c, \omega)} \\
&= 0
\end{aligned}
\tag{25}
$$

$$
\begin{aligned}
\begin{vmatrix}
p_{122,11} & p_{122,12} & p_{122,13} & p_{122,14} \\
p_{122,21} & p_{122,22} & p_{122,23} & p_{122,24} \\
p_{122,31} & p_{122,32} & p_{122,33} & p_{122,34} \\
p_{122,41} & p_{122,42} & p_{122,43} & p_{122,44}
\end{vmatrix}
&= f_{122(\beta_c, \lambda_c, \omega)} \\
&= 0
\end{aligned}
\tag{26}
$$

By adding the condition that β_c, λ_c and ω be real numbers in Equation 26, the values of β_c, λ_c and ω are determined

for given values of θ and d_s. By substituting them into Equation 25, $W_{(t)}$ is obtained. The value of $W_{(t)}$ at $t = 0$ is 1. That is, $W_{(t)}$ will be determined by linear analysis. When $d_{111} = 1$ and $d_{122} = 1$ in Equations 23 and 24, amplitudes on the first order, namely u_{111}, v_{111}, h_{111}, u_{122}, v_{122} and h_{122} are calculated for each wave.

Regarding the order $\varepsilon^{2/2}$ (the second order), equations in the same form as Equations 23 and 24 are obtained for the components of waves which have transverse and longitudinal numbers of wave modes (1, 1), (1, 3), (2, 2), (3, 1), (3, 3), (4, 4), (2, 0), (4, 0), (0, 2), (0, 4) and (0, 0) respectively.

$$\begin{bmatrix} p_{2ij,11} & p_{2ij,12} & p_{2ij,13} & p_{2ij,14} \\ p_{2ij,21} & p_{2ij,22} & p_{2ij,23} & p_{2ij,24} \\ p_{2ij,31} & p_{2ij,32} & p_{2ij,33} & p_{2ij,34} \\ p_{2ij,41} & p_{2ij,42} & p_{2ij,43} & p_{2ij,44} \end{bmatrix} \begin{bmatrix} u_{2ij} \\ v_{2ij} \\ h_{2ij} \\ d_{2ij} \end{bmatrix} = q_{2ij} \tag{27}$$

where, i, j = the transverse and longitudinal wave mode of small perturbation. These equations, however, are nonhomogenous, which means that the right-hand side of each equation exceeds zero. Thus, amplitudes on the second order can be obtained for u_{211} and other values of the second order by using the values obtained on the first order.

The same order can be applied to the waves of (1, 1) and (2, 2), which represent an alternate bar and a double-row bar, respectively. Therefore, when the perturbation parameter for nonlinear analysis is ε, it is theoretically possible to determine $A_{(T)}$ and $B_{(T)}$, which represent bar formation processes on the second order, and Equations 28 and 29 are obtained.

$$\frac{dA_{(T)}}{dT} + \alpha_1 A_{(T)} + \alpha_2 B_{(T)} \overline{A}_{(T)} = 0 \tag{28}$$

$$\frac{dB_{(T)}}{dT} + \alpha_4 B_{(T)} + \alpha_5 {A_{(T)}}^2 = 0 \tag{29}$$

However, each equation diverges over time when they are used for calculation under the conditions of hydraulic tests described below. Therefore, nonlinear analysis was repeated with a perturbation parameter of $\varepsilon^{1/2}$. When waves which have the transverse and longitudinal modes of (1, 1) and (2, 2) are subjected to the above on the order of $\varepsilon^{3/2}$ (the third order), then Equations 30 and 31 are obtained.

$$\frac{dA_{(T)}}{dT} + \alpha_1 A_{(T)} + \alpha_2 {A_{(T)}}^2 \overline{A}_{(T)} + \alpha_3 A_{(T)} B_{(T)} \overline{B}_{(T)} = 0 \tag{30}$$

$$\frac{dB_{(T)}}{dT} + \alpha_4 B_{(T)} + \alpha_5 {B_{(T)}}^2 \overline{B}_{(T)} + \alpha_6 B_{(T)} A_{(T)} \overline{A}_{(T)} = 0 \tag{31}$$

If these equations are solved simultaneously, the values $A_{(T)}$ and $B_{(T)}$ are obtained. Analytical solutions, however, are impossible, and thus numerical calculation is used. $W_{(t)}$ are included in the coefficients α_1 to α_6. The fourth term on the left side of Equations 30 and 31 represents cross interference and these equations have the same form as Equation 15 when the fourth term is omitted.

A COMPARISON BETWEEN NONLINEAR ANALYSIS RESULTS AND HYDRAULIC TEST RESULTS

The bedload and the coefficient of riverbed resistance used for analysis are represented by Equations 32 and 33 below, which are respectively the equations of Meyer-Peter & Müller, and of Engelund & Hansen.

$$\phi = 8\,(\theta - \theta_{cr})^{3/2} \tag{32}$$

Table 2: Hydraulic conditions of experiments, initial conditions of analysis and calculated results of amplitude.

Run	β	d_s	θ	$A_{(0)}$	$B_{(0)}$	β_c	$\varepsilon^{1/2}$	${F_0}^2 h_{111} - d_{111}$	${F_0}^2 h_{122} - d_{122}$
S-30	37.5	0.063	0.12	0.0065	0.0010	17.5	1.07	-0.853 - 0.0814 i	-0.859 - 0.0426 i
S-40	30.0	0.051	0.15	0.0020	0.0010	18.5	0.79	-0.853 - 0.0823 i	-0.860 - 0.0431 i
S-50	25.0	0.042	0.18	0.0010	0.0010	19.2	0.55	-0.855 - 0.0807 i	-0.862 - 0.0423 i

$$C_f = \frac{1}{\left[6 + 2.5 \ln\left(\frac{D}{2.5 d_s}\right)^2\right]} \tag{33}$$

where, ϕ = dimensionless bedload transport rate for a unit width; and θ_{cr} = dimensionless critical shear stress. Both equations reproduce the test results accurately and thus can be used for analysis without problems (Watanabe & Kuwamura (10)).

In solving Equations 30 and 31, the values shown in Table 2 were used as the initial values for $A_{(T)}$ and $B_{(T)}$. These initial values are discussed in detail in the next section.

In Figure 6, the observed amplitudes α_{11} and α_{22} are compared with the calculated amplitudes. The calculated amplitude α_{11} and α_{22} are obtained by Equations 34 and 35.

$$\alpha_{11} = \left|A_{(T)} W_{(t)} \left({F_0}^2 h_{111} - d_{111}\right)\right| \tag{34}$$

$$\alpha_{22} = \left|B_{(T)} \left({F_0}^2 h_{122} - d_{122}\right)\right| \tag{35}$$

The amplitude α_{11} is for the wave that has the wave mode of 1 in the transverse and longitudinal directions; (1,1), and α_{22} is the amplitude of the wave that has the wave mode of 2 in the transverse and longitudinal directions; (2,2). The observed amplitude was obtained by a wavenumber analysis applied to the riverbed configuration identified in the hydraulic tests. $\left|A_{(T)} W_{(t)} \left({F_0}^2 h_{111} - d_{111}\right)\right|$ is a calculated amplitude of the wave that has a wave mode (1,1) and $\left|B_{(T)} \left({F_0}^2 h_{122} - d_{122}\right)\right|$ is a calculated amplitude of the wave that has the wave mode (2,2). The calculated amplitude was obtained by the weakly nonlinear analysis. The calculated values of amplitude are larger than the experimental values. However, as the width/depth ratio increases, the amplitude tends to become smaller, and the general tendency of transition from double-row bars to alternate bars is represented well, especially after the initial increase in amplitude of both types of bars. These amplitudes are expressed in values relative to the observed equilibrium amplitude of α_{11}, α_{11e}, for confirming the changes with time clearly. Then, Figure 6 is rewritten as Figure 7. Particularly well represented is the attenuation with time in the components of double-row bars, whose wave mode is (2,2).

In the analysis on the second order, waves which have the longitudinal and transverse wave modes of 1 and 2, expressed as $\left|\overline{A}_{(T)} \overline{W}_{(t)} B_{(T)} \left({F_0}^2 h_{211} - d_{211}\right)\right|$ for wave mode (1,1) and $\left|{A_{(T)}}^2 {W_{(t)}}^2 \left({F_0}^2 h_{222} - d_{222}\right)\right|$ for wave mode (2,2), appear. These waves should be taken into consideration, and the calculated heights of sandbars are compared with the hydraulic test results in Figure 8. It can be observed that solutions oscillate with time as the perturbation parameter $\varepsilon^{1/2}$ grows. This may suggest, as Pornprommin et al. (6) propose, that the oscillation of the amplitude increases when the width/depth ratio becomes large. But the time change in the value of $\left|W_{(t)}\right|$ for S-40 shown in Figure 9 suggests that $\left|W_{(t)}\right|$ tends to diverge with time. It is possible that this oscillation results from the method used in this study. Moreover, although the method is originally formulated for phenomena that take place near the growth rate of 0, the linear growth rate $W_{(t)}$ was applied in this study. At the same time, a discrepancy might arise as a result of applying the method to a region which has a relatively large growth rate. It is also shown that each wave expressed in the equation does not diverge but instead maintains a steady value, despite $W_{(t)}$ having a relatively large value. The discrepancy found in this study needs to be addressed.

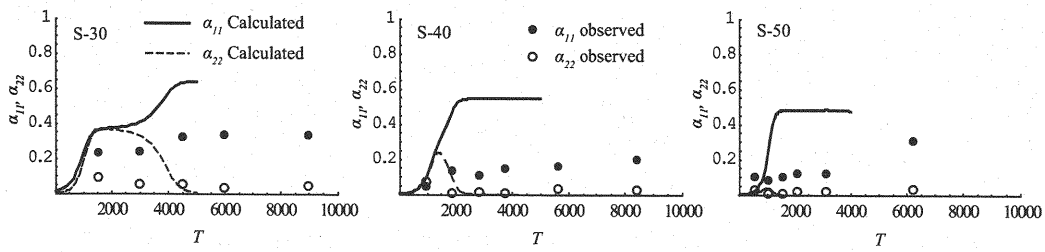

Figure 6: Experimental values and calculated solutions on the first order: temporal changes in the components of alternate bars and double-row bars.

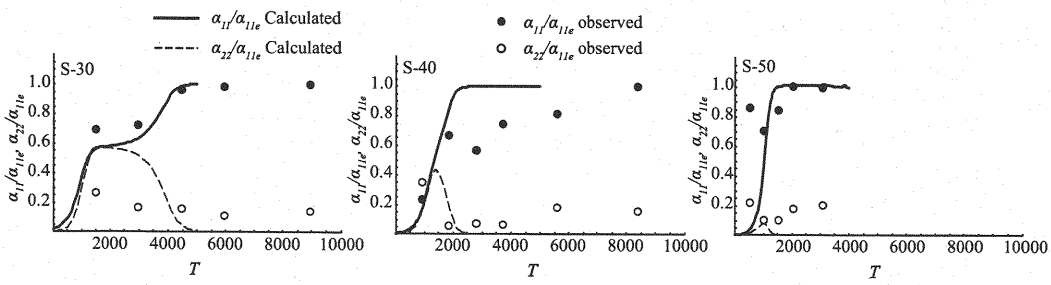

Figure 7: Experimental values and calculated solutions on the first order: temporal changes in the standardized components of alternate bars and double-row bars by the observed equilibrium amplitude of α_{11}, α_{11e}.

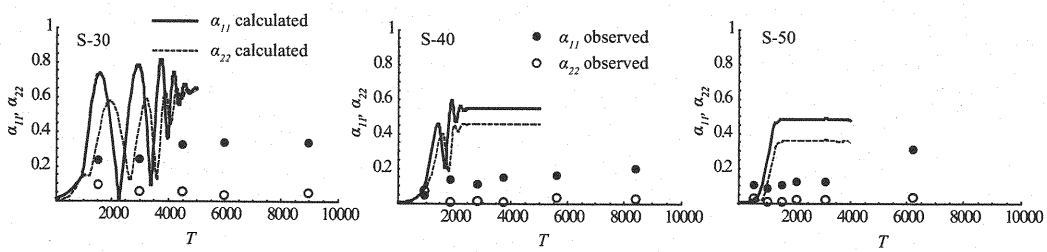

Figure 8: Experimental values and calculated solutions (on the first order and the second order): temporal changes in the components of alternate bars and double-row bars

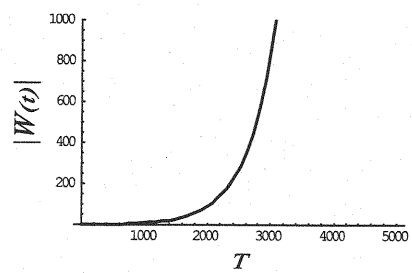

Figure 9: Temporal change of linear growth rate $|W_{(t)}|$ for S-40.

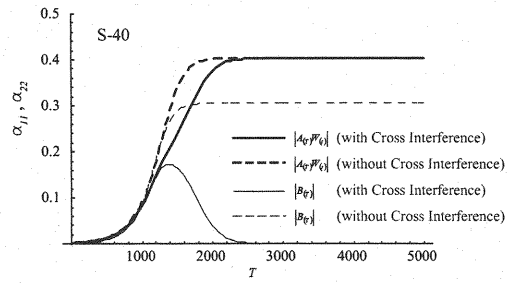

Figure 10: Influence of cross interference to bar amplitude in case of S-40.

While the above irregularity needs to be solved, a comparison between the results of Figure 6, Figure 7 and Figure 8 shows that the analysis results conform to test results (Watanabe & Kuwamura (9)). Even when the amplitude $\left|A_{(T)}W_{(t)}\left(F_0{}^2h_{111}-d_{111}\right)\right|$ of the wave which has a wave mode (1,1) on the fist order increases and the amplitude $\left|B_{(T)}\left(F_0{}^2h_{122}-d_{122}\right)\right|$ of the wave which has a wave mode (2,2) on the first order decreases, the amplitude $\left|A_{(T)}{}^2W_{(t)}{}^2\left(F_0{}^2h_{222}-d_{222}\right)\right|$ of the wave which has the wave mode (2,2) on the second order grows and the characteristics of a double-row bar are maintained.

DISCUSSION ON MODE DECREASE PROCESS

The characteristics of the transition from double-row bars to alternate bars are reproduced satisfactorily by this weakly nonlinear analysis. The mode cross interference working in a process of mode reduction from double-row bars to alternate bars is examined on the basis of the results of this analysis.

The results of hydraulic test S-40 are used, because in S-40 the mode reduction from double-row bars to alternate bars is clearly shown and a perturbation parameter $\varepsilon^{1/2}$ is the smallest in the experiments which the mode reduction was generated.

Cross Interference to Bar Amplitude

Figure 10 shows the influence of cross interference to the amplitude of bars. The solid lines show the developing processes of $\left|A_{(T)}W_{(t)}\right|$ and $\left|B_{(T)}\right|$ considering with the cross interference. The dashed lines show the results without cross interference. There is evidence that the development process of $\left|A_{(T)}W_{(t)}\right|$ and $\left|B_{(T)}\right|$ is strongly influenced of cross interference when these lines are compared. $\left|B_{(T)}\right|$ is decreased to 0 after progressed to some extent, and $\left|A_{(T)}W_{(t)}\right|$ reaches at an equilibrium height as same that without cross interference, although rather late because of the cross interference. The mode cross interference controls the development process of each wave.

Difference in time change of each amplitude by the initial value

Figure 11(a) shows the temporal changes in $\left|A_{(T)}W_{(t)}\right|$, $\left|B_{(T)}\right|$, $\left|\overline{A}_{(T)}\overline{W}_{(t)}B_{(T)}\right|$ and $\left|A_{(T)}{}^2W_{(t)}{}^2\right|$ when the initial values of $A_{(T)}$ and $B_{(T)}$ are given 0.002 and 0.001, respectively. This means that $A_{(T)}$ exceeds $B_{(T)}$ in the early stages of development process. While $\left|B_{(T)}\right|$ grows in the early stages of water flow just as $\left|A_{(T)}W_{(t)}\right|$ does, it begins to attenuate when $\left|A_{(T)}W_{(t)}\right|$ grows to some level. This is in line with the results of the hydraulic tests.

Table 3: Initial conditions of $A(T)$ and $B(T)$ of analysis

Case	$A(0)$	$B(0)$	Case	$A(0)$	$B(0)$
I-1	0.000022	0.00001	II-1	0.000021	0.00001
I-2	0.001	0.00001	II-2	0.00001	0.0001
I-3	0.01	0.00001	II-3	0.00001	0.01

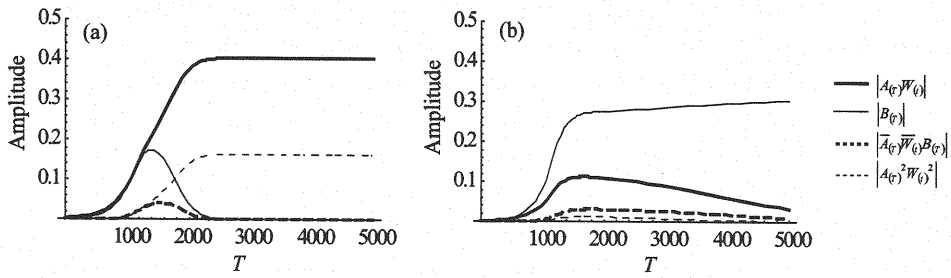

Figure 11: Difference in temporal changes in amplitude by different initial values: (a) $A_{(0)} = 0.002$ and $B_{(0)} = 0.001$; (b) $A_{(0)} = 0.001$ and $B_{(0)} = 0.001$.

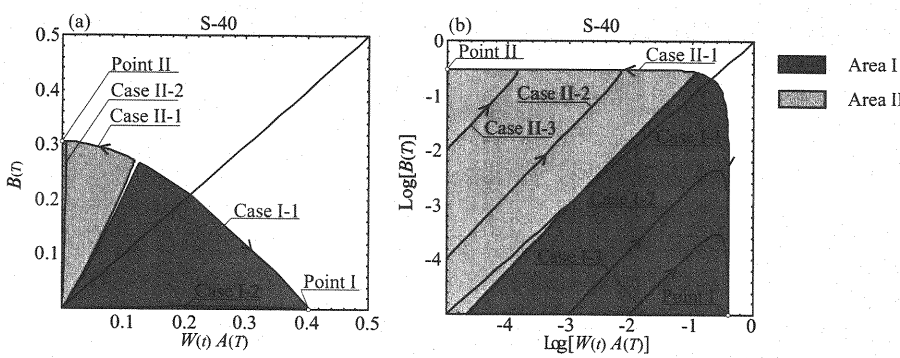

Figure 12: the development processes of $W(t)A(T)$ and $B(T)$ by the different initial values

Figure 11(b) shows the results when the initial value is set at 0.001 for both $A_{(T)}$ and $B_{(T)}$. In this case, the results of our analysis differ from the hydraulic test results: $|A_{(T)}W_{(t)}|$ attenuates, but $|B_{(T)}|$ keeps on growing.

Thus, the results shown in Figure 11(a) and (b) indicate that different initial values result in different tendencies. The same figures show that on the first order only one mode can grow. This can also be interpreted to mean that the mode cross interference is almost unilateral and that one mode cannot grow when the other mode is predominant. In Figure 11(b), $|A_{(T)}W_{(t)}|$ and $|B_{(T)}|$ have a tendency to decrease or increase, respectively. As a time proceeds, $|A_{(T)}W_{(t)}|$ goes to 0 and $|B_{(T)}|$ changes to a constant value.

The developing processes of $|A_{(T)}W_{(t)}|$ and $|B_{(T)}|$ with the combination of various initial conditions are investigated. The initial conditions of each case are summarized in Table 3. Figure 12 (a) is the parametric plot on $|A_{(T)}W_{(t)}|$ and $|B_{(T)}|$ using hydraulic condition of S-40. Figure 12 (b) is transformed into logarithmic axes using the same data. These figures show that either of $|A_{(T)}W_{(t)}|$ and $|B_{(T)}|$ can survive at the equilibrium stage. When the initial values are in Area I, the equilibrium stage is shown as Point I and only $|A_{(T)}W_{(t)}|$ survives, and when these are in Area II, the equilibrium stage is shown as Point II and only $|B_{(T)}|$ survives. Arrows in the figures show the direction of the development process. In the case of S-40, Area I is larger than Area II. This result reveals that only the phenomenon which shifts to alternate bars from double-row bars can be confirmed. However, a different

result from the actual phenomenon is predicted when the initial values of $A(T)$ and $B(T)$ are made too small. It is necessary to use suitable initial values for this theory.

CONCLUSIONS

In this study, a weakly nonlinear analysis, which can represent mode cross interference, was conducted to understand phenomena in reduction of mode from double-row bars to alternate bars. Although there are some problems in terms of quantitative evaluations and basis for setting initial values of perturbation, the characteristics of the mode reduction process are qualitatively reproduced. The following findings were obtained from our theoretical analysis. The development process of bars is strongly influenced of the mode cross interference. Findings show that when the two modes are on the same order, the mode cross interference controls development process of each wave and they cannot grow simultaneously. In order to reproduce the mode decrease process of bars by the weakly nonlinear analysis, it is necessary to use the suitable initial values of perturbation. Evidence shows that the solutions bifurcate by the initial values. However, the stability of each solutions has to be considered and further study on the stability is needed.

ACKNOWLEDGEMENTS

We would like to thank the Hokkaido Regional Development Bureau of the Ministry of Land, Infrastructure and Transport, for commissioning CERI with this work; the Foundation of River and Watershed Environment Management, for a grant; and the Japan Society for the Promotion of Science, for research aid (Basic research (B) (1) 16360242).

REFERENCES

1. Colombini, M., Seminara, G. & Tubino, M. : Finite amplitude alternate bars, Journal of Fluid Mechanics Vol.181, pp.213-232,1987.

2. Fujita, Y. : Bar and channel formation in braided streams, In Ikeda, S. & Parker, G. (eds), River meandering, Water Resource Monograph 2, pp.417-462, 1989.

3. Fujita, Y., Nagata, N. & Muramoto, Y. : Formation process of braided stream, Annual Journal of Hydraulic Engineering of JSCE, Vol.36, pp.23-28, 1992 (in Japanese with English abstract).

4. Izumi, N. & Pornprommin, A. : Weakly nonlinear analysis of bars with the use of the amplitude expansion method, Journal of hydraulic, coastal and environmental engineering, No.712/II-60, JSCE, pp.73-86, 2002 (in Japanese with English abstract).

5. Schielen, R., Doelman, A. & de Swart, H. E. : On the nonlinear dynamics of free bars in straight channels, Journal of Fluid Mechanics, Vol.252, pp.325-356, 1993.

6. Pornprommin, A., Izumi, N. & Tsujimoto, T. : Weakly nonlinear analysis of multimodal fluvial bars, Annual Journal of Hydraulic Engineering, Vol.48, JSCE, pp.1009-1014, 2004.

7. Takebayashi, H., Egashira, S. & Okabe, T. : Stream formation process between confining banks of straight wide channels, Proceedings of the 2nd IAHR Symposium on River, Coastal and Estuarine Morphodynamics, pp.575-584, 2001.

8. Teramoto, A. & Tsujimoto, T. : Effects of size heterogeneity of bed materials on mechanism to determine bar mode, Proceedings of the 4th IAHR Symposium on River, Coastal and Estuarine Morphodynamics, pp.433-444, 2005.

9. Watanabe, Y. & Kuwamura, T. : Experimental study on mode reduction process of double-row bars, Annual Journal of Hydraulic Engineering, Vol.48, JSCE, pp.997-1002, 2004 (in Japanese with English abstract).

10. Watanabe, Y. & Kuwamura, T. : Mode-decrease process of double-row bars, Proceedings of the 4th IAHR Symposium on River, Coastal and Estuarine Morphodynamics, pp.445-453, 2005.

APPENDIX - NOTATION

The following symbols are used in this paper:

$A_{(T)}$	=	the amplitude of small perturbation at time T;
$\overline{A}_{(T)}$	=	the complex conjugate of $A_{(T)}$;
$\widetilde{B}$	=	half the channel width;
$c.c.$	=	the complex conjugate of the immediately preceding term;
C_f	=	drag coefficient of riverbed;
d_s	=	$\widetilde{d_s}/\widetilde{D_0}$ (dimensionless grain size);
$\widetilde{d_s}$	=	diameter of bed material;
$\widetilde{D}$	=	local water depth;
$\widetilde{D_0}$	=	average water depth;
$\widetilde{g}$	=	acceleration of gravity;
$h.h.$	=	a term of high order;
$\widetilde{H}$	=	water level;
I_b	=	bed slope;
I_w	=	water gradient;
$\widetilde{L_b}$	=	the average wavelength;
m	=	the mode number for transverse direction of bar formation;
n	=	the mode number for longitudinal direction of bar formation;
p	=	element of matrix and determinant;
P	=	porosity of bed;
$\widetilde{Q}$	=	discharge;
$\widetilde{Q_{bx}}$	=	bedload transport rate in the $\widetilde{x}$ coordinate direction;
$\widetilde{Q_{by}}$	=	bedload transport rate in the $\widetilde{y}$ coordinate direction;
t	=	the time scale of flow;
$\widetilde{t}$	=	time;
T	=	a time scale introduced to express the variation of small perturbation;
$\widetilde{T_f}$	=	duration;

$\widetilde{U}$ = flow velocity in the $\widetilde{x}$ coordinate direction;
$\widetilde{V}$ = flow velocity in the $\widetilde{y}$ coordinate direction;
$\widetilde{x}$ = longitudinal coordinate;
$\widetilde{y}$ = transverse coordinate;
Z_b = $\widetilde{Z_b}/\widetilde{D_0}$;
$\widetilde{Z_b}$ = wave height of sandbars;
β = $\widetilde{B}/\widetilde{D_0}$;
β_c = the critical width/depth ratio for generating bars;
δ = the submerged specific gravity of the riverbed material;
$\varepsilon^{1/2}$ = perturbation parameter;
$\widetilde{\eta}$ = riverbed elevation ($= \widetilde{H} - \widetilde{D}$);
θ = dimensionless shear stress;
θ_{cr} = the dimensionless critical shear stress;
λ = $2\pi\widetilde{B}/\widetilde{L_b}$;
ϕ = the dimensionless bedload transport rate for a unit width;
$\widetilde{\rho}$ = density of water;
$\widetilde{\tau_x}$ = shear stress in the $\widetilde{x}$ coordinate direction; and
$\widetilde{\tau_y}$ = shear stress in the $\widetilde{y}$ coordinate direction.

(Received September 6, 2006 ; revised December 7, 2006)